Surface Morphology Dynamics in Strained Epitaxial InGaAs

T. Pinnington, C. Lavoie,* T. Tiedje,† B. Haveman, and E. Nodwell

Advanced Materials and Process Engineering Laboratory, Department of Physics and Astronomy, University of British Columbia, Vancouver, British Columbia, Canada V6T 1Z4

(Received 5 December 1996)

Elastic light scattering has been used to measure the time evolution of the power spectrum of the surface morphology of strained InGaAs layers during growth. From a combination of fixed scattering angle measurements during growth and variable scattering angle measurements after growth, we are able to determine both the time and spatial frequency dependence of the power spectral density during relaxation of the strained films via misfit dislocations. The data are fit with an Edwards-Wilkinson model, for which the surface morphology is driven by inhomogeneous surface strains. [S0031-9007(97)03924-0]

PACS numbers: 68.55.Jk, 61.16.Ch, 78.35.+c, 81.15.Hi

Computer simulations and analytical theory have contributed greatly to our understanding of the dynamical behavior of surface morphology during thin film growth. Experimental studies have been less definitive however. For example, the general form of the equations that describe surface morphology in the continuum limit is known from theory [1], yet experimental tests of these theories have tended to be limited to studies of the scaling relations for the interface width. The systems for which thin film growth is best understood are single crystal semiconductor films of Si, SiGe, and III-V semiconductors [2–5]. In this paper we use laser light scattering (LLS) to explore the dynamics of surface morphology in one of these systems, namely, strained InGaAs on GaAs, and compare the results with the predictions of the continuum growth models.

Electron diffraction techniques, which are the most commonly used surface structure probes, are not sensitive to the large scale structures of interest in studies of morphology in the continuum limit, due to the short coherence length of the electrons. Laser light scattering does not have this problem. For the mirrorlike substrates used in crystal growth experiments, LLS can detect atomic-scale changes in the surface height on lateral length scales comparable to an optical wavelength [6]. In addition to being highly sensitive, LLS is well suited to *in situ* measurements during growth [6,7]. A potential problem is that light scattering is sensitive to particles and point defects on the surface, which are difficult to distinguish from the scattering due to the surface morphology. However, by comparing light scattering results with atomic force microscope (AFM) measurements, we have found that LLS provides reliable quantitative morphology information [8]. In addition, the scattering considered in this paper is highly anisotropic, indicating that it is dominated by the crosshatched morphology of the surface and not by the isotropic scattering expected from particles.

Light scattering measurements were carried out in a VG V80H molecular beam epitaxy (MBE) chamber [6], with a 27 mW, 488 nm Ar^+ laser incident normal to the substrate. The diffusely scattered light was detected simultaneously at 25° and 55° from the surface normal. The sample orientation was fixed during growth such that the plane of scattering defined by the detector ports coincided with the $[1\bar{1}0]$ direction in the plane of the substrate surface. For this geometry the scattered light is sensitive to surface height fluctuations along the $[1\bar{1}0]$ direction with spatial frequencies q of 5.4 and 10.5 μm^{-1} for the ports at 25° and 55°, respectively. The incident laser beam spot was about 2 mm in diameter on the surface of the sample and was located at a position with no defects or particles visible in the laser spot.

The as-received (001)-oriented (±0.5°) GaAs substrates were cleaned by exposure to uv ozone for 5 min in a laminar flow hood followed by thermal desorption of the surface oxide under an arsenic overpressure in the MBE growth chamber. A 1 μm thick GaAs buffer layer was grown at 590 °C at a growth rate of 1 μm/h. Before termination of the buffer layer growth the substrate temperature was ramped down to 490 °C for the InGaAs growth. The As_2 to Ga flux ratio was 3.5:1 and these fluxes were held constant throughout growth of the GaAs and InGaAs layers. In order to preserve the surface morphology for *ex situ* measurements, the substrate heater power was turned off immediately after growth. This procedure causes the substrate temperature to drop below 300 °C within 5 min by radiative cooling to the liquid nitrogen cryoshroud, as measured by diffuse reflectance spectroscopy [9]. The scattered light signal was found to remain stable during the quench.

In Fig. 1(a) we show a 50×50 μm^2 AFM image of a 250 nm thick $In_{0.18}Ga_{0.82}As$ film. This image shows the well-known $\langle 110 \rangle$ crosshatch pattern which is observed in relaxed InGaAs films. We note that the ridges which make up the crosshatch pattern are 1 to 3 nm high, which is considerably higher than the atomic-size steps one would expect from slip along $\langle 111 \rangle$ planes associated with individual misfit dislocations. These

 0031-9007/97/79(9)/1698(4)$10.00 © 1997 The American Physical Society

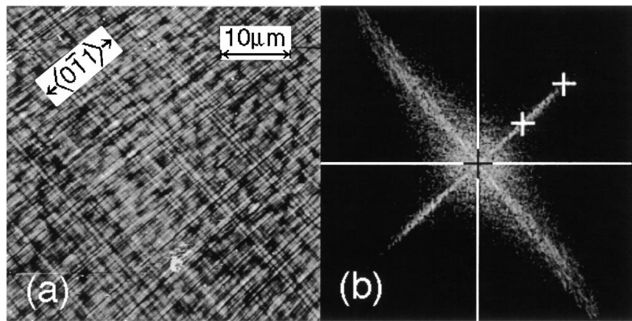

FIG. 1. (a) AFM image of a 250 nm thick InGaAs film, with a 5 nm vertical gray scale and (b) power spectrum calculated from the AFM image, where the gray scale represents the logarithm of the PSD at each spatial frequency q. The axes for the PSD are oriented approximately along $\langle 001 \rangle$ directions and span a q range of ± 16 μm^{-1} ($q = 0$ at origin). The white crosses show the spatial frequencies monitored in Fig. 2.

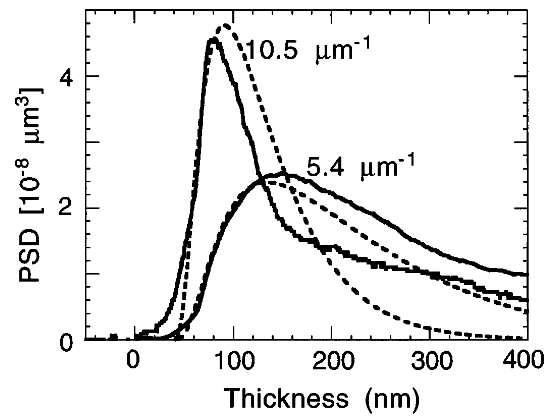

FIG. 2. *In situ* light scattering measurements (solid lines) of surface roughness at $q = 5.4$ and 10.5 μm^{-1} during growth of an InGaAs film, and calculated time evolution of the 1D PSD (dotted lines).

ridges are believed to be caused by surface diffusion in response to the inhomogeneous strain associated with the misfit dislocations [5,7,10]. The two-dimensional power spectrum obtained by Fourier transforming the image data is shown in Fig. 1(b). The $\langle 110 \rangle$ cross pattern in the power spectral density (PSD) means that the scattered light intensity, which is proportional to the PSD of the surface height [11], should be concentrated in two orthogonal directions parallel to the $\langle 110 \rangle$ crystal axes. There is an angular spread in the cross pattern due to distortion in the AFM scan; however, the corresponding scattering lines are one dimensional (1D), with a width determined by the divergence of the laser beam. To detect the light scattered in these directions during growth, it is critical to align the scattering planes accurately along the $\langle 110 \rangle$ directions in the substrate at the beginning of the experiment.

In addition to the 1D roughness associated with the crosshatch pattern there is a 2D background roughness consisting of mounds elongated along the $[1\bar{1}0]$ direction, which produces the oval-shaped intensity distribution in the power spectrum, elongated along $[110]$. The rms value of this background roughness is 1 nm. The mounds develop during growth of the GaAs buffer layer [3] and persist during growth of the InGaAs layer. The elliptical shape of mounds reflects the asymmetry in surface diffusion in the two $\langle 110 \rangle$ directions on GaAs [12].

The scattered light intensity during growth of a strained InGaAs film is shown in Fig. 2. The detected light signals probe lateral length scales ($2\pi/q$) of 1.2 and 0.6 μm in the crystal surface. The background scattering signal (about 10% of the peak intensity) associated with the residual 2D roughness of the GaAs buffer layer has been subtracted from both curves. This is the 2D scattering which falls into the solid angle of the detector along with the 1D scattering. There is a sharp increase in scattering along the $[1\bar{1}0]$ direction when the film is about 40 nm thick. *Ex situ* structural analyses on these films showed that the surface roughening coincides with the formation of misfit dislocations [6].

The $[1\bar{1}0]$ 1D power spectra determined from *ex situ* light scattering are shown in Fig. 3. The PSD as a function of q is proportional to the scattered light intensity as a function of $2\pi[\sin\theta_i - \sin\theta_s]/\lambda$, where θ_i and θ_s are the incident and scattering angles, respectively [11]. Here, a 632 nm HeNe laser was incident on the sample at 65°

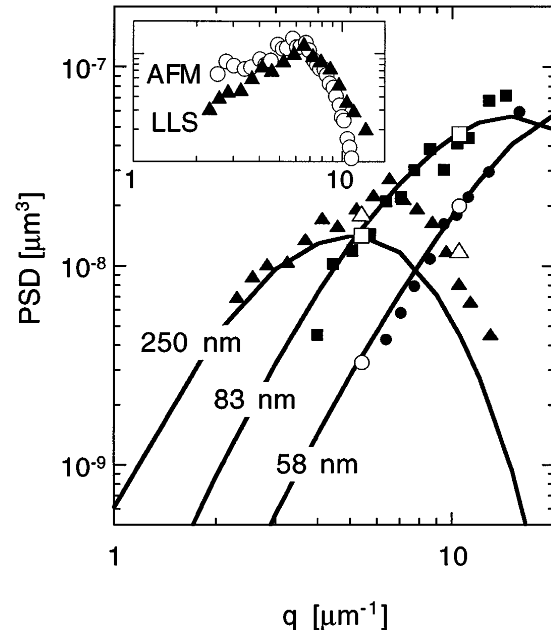

FIG. 3. *Ex situ* LLS (solid symbols) and model data (solid lines) for the 1D PSD of three InGaAs films with different thicknesses above the critical thickness. The corresponding *in situ* data from Fig. 2 are shown for reference (open symbols). The *ex situ* data for the 250, 83, and 58 nm thick films have been scaled by factors 1/4.5, 1.5, and 4.5, respectively, to match the *in situ* measurements. Inset: AFM and LLS measurements (unscaled) of the PSD of the 250 nm thick film plotted on the same scale.

from the normal. The scattered light was detected in the plane of incidence at backscattering angles ranging from 12° to 110° away from the specularly reflected light, corresponding to spatial frequencies from 1 to 16 μm^{-1}. The signal measured along [100], which is representative of the 2D background, was subtracted from the $[1\bar{1}0]$ data in order to isolate the 1D component of the surface roughness from the 2D component which falls within the detector solid angle. The 1D PSD obtained in this way agrees quantitatively with that determined from Fourier transforms of AFM data [8], as shown in the inset of Fig. 3.

The three sets of data in Fig. 3 were taken from films grown to different thicknesses under nominally the same conditions. The *ex situ* data showed a different thickness dependence than the *in situ* measurements in Fig. 2. Systematic errors in the *ex situ* measurements could be caused by differences in the samples due to imperfect run-to-run control over growth parameters. We believe that the measurements during growth of one sample are a more reliable measure of the thickness dependence of the PSD than measurements on several different films after growth. Similarly, the q dependence obtained from the *ex situ* measurements with one detector is more reliable than the q dependence obtained from measurements at different ports during growth. This is due mainly to variabilities in the *in situ* optical alignment and window coating (periscope ports were used to minimize coating) which we estimate can change the optical throughput by a factor of 2 or more.

Accordingly, the relative magnitudes of the *in situ* signals measured at two different optical ports in Fig. 2 were scaled by a factor of 1.7 to match the q dependence obtained *ex situ* on the 58 nm thick film (solid circles in Fig. 3). Similarly, the *ex situ* data for different thicknesses were scaled to match the *in situ* thickness dependence measured at $q = 5.4\ \mu\text{m}^{-1}$. The open symbols at 5.4 and 10 μm^{-1} in Fig. 3 indicate the relative intensities obtained from measurements during growth. The agreement between the open and solid symbols at 5.4 μm^{-1} is simply due to the fact that the q dependence is normalized to the open symbols at this point; however, the agreement at 10.5 μm^{-1} (triangle and square) is not due to normalization and is an indication of the internal consistency of the data.

During relaxation of these compressively strained films, 60° misfit dislocations (Burgers vector = $a/2\langle 101\rangle$) form at the substrate/epilayer interface with slip along {111} planes which intersect the interface along $\langle 110\rangle$ directions. The surface roughening in the relaxed films occurs along two orthogonal $\langle 110\rangle$ directions due to surface migration in response to the inhomogeneous strain field at the surface from the dislocation array. Roughening in the two directions is assumed to be independent and we neglect the contribution from the atomic steps produced where the slip planes intersect the surface. Plan view transmission electron microscopy (TEM) measurements on these films showed visually random $\langle 110\rangle$ misfit dislocations whose density was consistent with the film relaxation inferred from x-ray diffraction, to within a factor of 2 [13].

For an atom diffusing on the surface of a strained film, the change in the chemical potential $\mu(x,t)$ produced by the local strain field $\varepsilon(x,t)$ at position x and time t can be linearized as follows:

$$\mu(x,t) \approx \frac{Y\Omega}{2}\left[-\bar{\varepsilon}^2(t) + 2\bar{\varepsilon}(t)f + 2\bar{\varepsilon}(t)\delta_\varepsilon(x,t)\right], \quad (1)$$

where the local deviation in the strain field $\delta_\varepsilon(x,t)$ is assumed to be small compared to the average strain $\bar{\varepsilon}(t)$. Y is the biaxial modulus, Ω is the volume of the unit cell and f is the initial in-plane strain due to the lattice mismatch. The contribution of shear strain produced by the mixed screw/edge dislocations is of order $(\delta_\varepsilon)^2$ and is neglected. The following equation can be used to describe the time evolution of the surface height distribution, $h(x,t)$ [1]:

$$\frac{\partial h(x,t)}{\partial t} - \nu\nabla^2 h(x,t) = \frac{\Omega DnY}{kT}\,\bar{\varepsilon}(t)\nabla^2\delta_\varepsilon(x,t), \quad (2)$$

where we have included a surface-gradient-driven current equal to $\nu\nabla h$. We take $\nu > 0$ which ensures stable growth [1]. D is the surface diffusion coefficient, and n is the concentration of diffusing atoms. The contribution of the elastic strain to the chemical potential is included, and the contribution of the surface curvature is neglected. To include the curvature one would need to add a $\nabla^4 h$ term to Eq. (2) [14]. $\delta_\varepsilon(x,t)$ is determined by summing the contributions to the surface strain at x from all dislocations present at the interface at time t neglecting interactions between dislocations. The strain field $\varepsilon_1(x,z)$ at the surface due to a single interfacial misfit with Burgers vector b, located at $x = 0, z = 0$, is [5]

$$\varepsilon_1(x) = -\frac{bz}{\pi}\,\frac{(x^2 - \sqrt{2}\,xz)}{(x^2 + z^2)^2} \Leftrightarrow \frac{b}{2}\,e^{-z|q|}(z|q| - 1 + i\sqrt{2}\,z|q|), \quad (3)$$

where $\Leftrightarrow$ denotes Fourier transform, q is the spatial frequency, and z is the film thickness. We assume that the dislocations in the 1D array are randomly distributed with average linear density $\rho(t)$. In this case the Fourier transform of $\delta_\varepsilon(x,t)$ is $\hat{\delta}_\varepsilon(q,t) = \sqrt{2\rho(t)}\,\hat{\varepsilon}_1(q,z)$. Solving the Fourier transform of Eq. (2) we find

$$\hat{h}(q, z + z_r) = Aq^2 e^{-\nu q^2 z/g}\int_0^{z/z_r - 1} e^{\nu q^2 \zeta z_r/g}\,\bar{\varepsilon}\rho^{1/2}\hat{\varepsilon}_1(q, z_r(\zeta + 1))\,d\zeta, \quad (4)$$

where $A = (\sqrt{2}\,z_r\Omega^2 DnY)/(gkT)$, g is the growth rate, and z_r is the thickness at which the film begins to relax. We have used a $1/z$ dependence for the residual strain above z_r: $\bar{\varepsilon}(z) = (fz_r)/z$, where $z = gt$. This is equivalent to the Matthews-Blakeslee model [15] if a logarithmic term is neglected, and is consistent with recent *in situ* measurements of

strain in this system [16]. The average dislocation density $\rho(z)$ is linearly related to the relieved strain through the in-plane component of the Burgers vector: $\rho = 2(f - \overline{\varepsilon})/b$; for $z < z_r$, $\rho = 0$.

The PSD obtained by integrating Eq. (4) numerically is fitted to the time-dependent light scattering data in Fig. 2, using the experimental growth rate (1 μm/h) and lattice mismatch ($f = 0.013$). In addition to the constant A, the calculated curves have two fitting parameters, namely, $\nu = 1.4 \times 10^{-12}$ cm^2/s and $z_r = 40$ nm. The same parameter values lead to the fits to the q-dependent data shown in Fig. 3.

The film thickness for maximum roughness and relative amplitudes of the surface roughness at different spatial frequencies calculated from the model approximately match the *in situ* measurements in Fig. 2. The model predicts that the roughness goes to zero faster for thick films than is observed experimentally, particularly at high spatial frequencies. This may be due to complicated dislocation structures not considered in the model, such as pileups, which are believed to act in the later stages of relaxation [7]. The fitted z_r is 4 times the Matthews-Blakeslee critical thickness. This is due to kinetic constraints on the nucleation of misfits which cause the experimental critical thickness measured during growth to exceed the equilibrium value, in agreement with others [7,16]. The small continuous increase in roughening below z_r in the experiment may be due to substrate threading dislocations bending over. Substantial strain relaxation does not occur until the film thickness exceeds the equilibrium critical thickness sufficiently to cause nucleation of large numbers of dislocations.

The calculated q dependence of the surface roughness agrees remarkably well with the q-dependent light scattering data in Fig. 3. The model shows the same trends with thickness as the experiment, with the same rising slope and a peak in the PSD at roughly 5 μm^{-1} for the thickest film. The roughness develops first at high spatial frequencies. This is expected because the surface topography will develop more rapidly at short length scales where a smaller amount of material needs to be transported a shorter distance to create the same amplitude on the surface. The high frequency roughness decreases at large thicknesses because the high frequency content of the surface strain field drops as the distance from the interface increases.

Run-to-run variations in ν due to small differences in composition, substrate off-cut, temperature, etc., have a larger effect on the amplitude of the PSD ($\propto \nu^{-2}$) than on the peak position ($\propto \nu^{-1/2}$ approximately). Thus a factor of 2 decrease in ν could explain the scale factor for the thickest film in Fig. 3, and shift the peak position from 5 to 7 μm^{-1}, in agreement with the data. Further experiments are needed to find out how ν depends on growth conditions.

In conclusion, we have used light scattering to obtain quantitative information on surface morphology during film growth, and not just relative values of surface roughness. This work is the first example of an experiment in which the predictions of a continuum growth equation have been compared with the time and spatial frequency dependence of the surface morphology of a growing film. For strained InGaAs on GaAs we find good agreement with the simplest equation, namely the Edwards-Wilkinson (EW) equation, in the 2–12 μm^{-1} spatial frequency range. STM studies have shown that MBE GaAs growth is unstable, in which case the EW equation should not be applicable. The good fit with the EW equation in the present case suggests that InGaAs growth is stable under our growth conditions.

We thank K. Kavanagh and S. Patitsas for useful discussions, and NSERC and Canadian Cable Labs for financial support.

---

*Current address: IBM Watson Research Center, Yorktown Heights, NY.

†Also at Department of Electrical Engineering, University of British Columbia, Vancouver, BC, V6T 1Z4.

[1] J. Villain, J. Phys. I (France) **1**, 19 (1991); F. Family, Physica (Amsterdam) **168A**, 561 (1990).
[2] Chung-Yu Mou and J.W.P. Hsu, Phys. Rev. B **53**, 7610 (1996); Z.H. Ming *et al.,* Appl. Phys. Lett. **67**, 629 (1995).
[3] C. Orme *et al.,* J. Cryst. Growth **150**, 128 (1995).
[4] A.G. Cullis, A.J. Pidduck, and M.T. Emeny, J. Cryst. Growth **158**, 15 (1996).
[5] F. Jonsdottir and L.B. Freund, Mech. Mater. **20**, 337 (1995). Equation (3) in the text is obtained from Eq. (6) of this reference in the limit of large dislocation spacing.
[6] C. Lavoie *et al.,* Appl. Phys. Lett. **67**, 3744 (1995); K.L. Kavanagh *et al.,* J. Cryst. Growth (to be published).
[7] R. Beanland and A.R. Boyd, in *Microscopy of Semiconducting Materials 1995,* edited by A.G. Cullis and A.E. Staton-Bevan, Inst. Phys. Conf. Series No. 146 (IOP, Bristol, 1995), p. 153.
[8] T. Pinnington, T. Tiedje, and C. Lavoie (to be published).
[9] S.R. Johnson, C. Lavoie, T. Tiedje, and J.A. Mackenzie, J. Vac. Sci. Technol. B **11**, 1007 (1993).
[10] G. Springholz, G. Bauer, and V. Holy, Phys. Rev. B **54**, 4500 (1996).
[11] E.L. Church, H.A. Jenkinson, and J.M. Zavada, Opt. Eng. **16**, 360 (1977).
[12] C. Lavoie *et al.,* Can. J. Phys. (Suppl.) **74**, S49 (1996).
[13] The thickest film looked at by TEM was 83 nm thick. In thicker films the average misfit spacing is less than the film thickness and it is no longer possible to be sure that they have distinct glide planes.
[14] We have done simulations in which the $\nabla^2 h$ term is replaced by $\nabla^4 h$. Comparably good fits could not be obtained with this equation.
[15] J.W. Matthews, S. Mader, and T.B. Light, J. Appl. Phys. **41**, 3800 (1970).
[16] P. Moeck *et al.,* in Proceedings of the 23rd International Conference on Phys. Semiconductors, edited by M. Scheffler and R. Zimmerman (World Scientific, Singapore, 1996), Vol. 2, p. 927.